Obtaining CBED Patterns

20

CHAPTER PREVIEW

We know that SAD, while giving us useful information about the specimen, has two severe limitations:

- We have to be very cautious in interpreting SAD patterns from areas which are less than ~0.5 μm in diameter. This size is large compared to the dimensions of many crystalline features that interest us in materials science (Chapter 16).
- SAD patterns contain only rather imprecise two-dimensional crystallographic information because the Bragg conditions are relaxed for a thin specimen and small grains within the specimen (Chapter 17).

D. B. Williams et al., *Transmission Electron Microscopy*

The technique of CBED overcomes both of these limitations and also generates much new diffraction information, which we will use in Chapter 21.

In this chapter we will show you how simple it is to use the versatility of modern (S)TEMs to create a range of CBED patterns containing a variety of contrast effects. We will also take you through the steps required to index the HOLZ spots and lines which occur under certain experimental conditions. In Chapter 21 you will see why these HOLZ features are so useful. They can give us an almost complete crystallographic analysis of the specimen. As is often the case in TEM, our advantage is that we have high spatial resolution. CBED, like many other sophisticated analytical techniques, uses various obscure definitions and acronyms which we will attempt to clarify as we introduce them.

Obtaining CBED Patterns

20

20.1. WHY USE A CONVERGENT BEAM?

Historically, CBED is the oldest TEM diffraction technique. It was originally developed by Kossel and Möllenstedt (1939) well before LePoole (1947) developed SAD. While SAD is the classical way to relate the diffraction-contrast information in the TEM image to the specimen orientation, it has a notable disadvantage. Remember we saw back in Chapters 9 and 11 that traditionally the diameter of the smallest area you can select by SAD is about 0.5 μm with an error of similar dimensions. However, if you have an intermediate voltage HRTEM with a very low C_s you may be able to use SAD to analyze areas ~0.1 μm in diameter. Many crystal defects and second-phase precipitates which influence the properties of materials are much smaller than this. As we've mentioned, one way we can overcome this limitation is to use a convergent beam of electrons (see Figure 9.4) to limit the region of the specimen which contributes to the DP. This region is a function of the beam size and beam–specimen interaction volume, which increases with specimen thickness but can be a lot smaller than in SAD. In fact, several so-called "microdiffraction" techniques have been developed to overcome the spatial-resolution limitations of SAD in a TEM. We'll review these techniques in Section 21.8. CBED is by far the most simple and versatile microdiffraction technique.

In addition to the improved spatial resolution, CBED gives us a wealth of new information not available in SAD, sometimes from a single DP. Such information comprises:

- Specimen thickness.
- Unit cell and precise lattice parameters.
- Crystal system and true 3D crystal symmetry (point group and space group).
- Enantiomorphism, if present.

With such capabilities, CBED has transformed electron diffraction from the "poor relative" of X-ray and neutron diffraction to a precise, and in some senses unique, diffraction technique.

> The big advantage of CBED over all other diffraction techniques is that most of the information is generated from minuscule regions beyond the reach of other diffraction methods.

In this chapter we will concentrate on how you can control the experimental variables to acquire and index CBED patterns; in the next chapter we will show you, among other things, how to perform what is known as "electron crystallography." In some materials we can even study scattering from within a unit cell. All these advantages can simultaneously be coupled with XEDS and EELS data, allowing you to achieve a remarkable degree of specimen characterization.

There are two potential drawbacks which you should always keep in mind:

- You may have local contamination which can cause localized stresses.
- The convergent beam may heat or damage the region of the specimen as you examine it.

In early probe-forming TEMs or those containing minilenses, you only had a few seconds to observe and record the CBED pattern before carbon contamination built up to a thickness which masked all the information. Modern TEMs should not suffer from this problem (see Chapter 8). Small regions of a clean specimen can be studied for minutes or even hours without visible contamination.

> Most specimen contamination is caused by the preparation process.

Beam heating/damage may be a problem in materials with poor thermal conductivity, but this can be mini-

mized by using a thin conductive carbon coating or preferably using a cooling holder. This latter approach has other advantages for CBED, as we'll see.

You may find that it is easier to use CBED rather than conventional SAD procedures. When reading the literature, remember that researchers often use the technique with which they are most familiar rather than the best one available.

20.2. OBTAINING CBED PATTERNS

First, which holder should you use? As with SAD you will need to do a lot of tilting so a double-tilt holder is required. Some of the diffraction phenomena we will be describing become more visible if the specimen is cooled to liquid-N_2 temperatures. If you want to carry out XEDS and CBED simultaneously then you'll also need a low-background holder. So a low-background, double-tilt, cooling holder is really useful. Tilt-rotation holders can sometimes be advantageous, but they are not available in a cooling or low-background form.

20.2.A. Comparing SAD and CBED

Now let's consider the differences in the electron optics of SAD and CBED. In SAD, the electron beam incident on the specimen is parallel (fixed incident vector **k**) and relatively large (usually ~1–10 μm in diameter). In CBED, the beam is convergent (range of **k**-vectors) and relatively small (usually ~10–100 nm in diameter), as shown in Figure 20.1. We have already seen in Chapters 11 and 16 that parallel illumination means that the SAD pattern consists of an array of sharp maxima in the back focal plane of the objective lens; Figure 20.2A shows such an SAD pattern from pure Si. In contrast, the beam convergence in CBED gives rise to a pattern of disks of intensity; Figure 20.2B is a CBED pattern from a much smaller region of the same Si specimen. While it isn't obvious that the CBED pattern comes from a smaller region of the specimen, you can certainly see that it contains a wealth of contrast detail not present in the SAD pattern. We'll see that, like SAD, CBED is most useful when the beam is oriented along a zone axis in the crystal, giving a symmetrical zone-axis (diffraction) pattern, commonly called a ZAP.

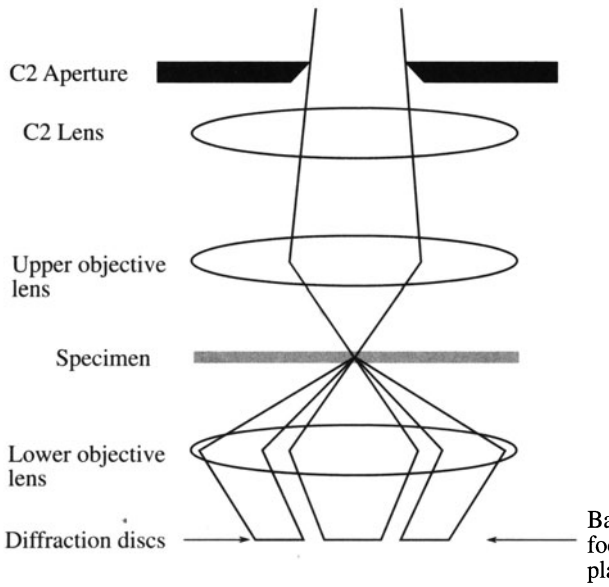

Figure 20.1. Ray diagram showing CBED pattern formation. A convergent beam at the specimen results in the formation of disks in the BFP of the objective lens.

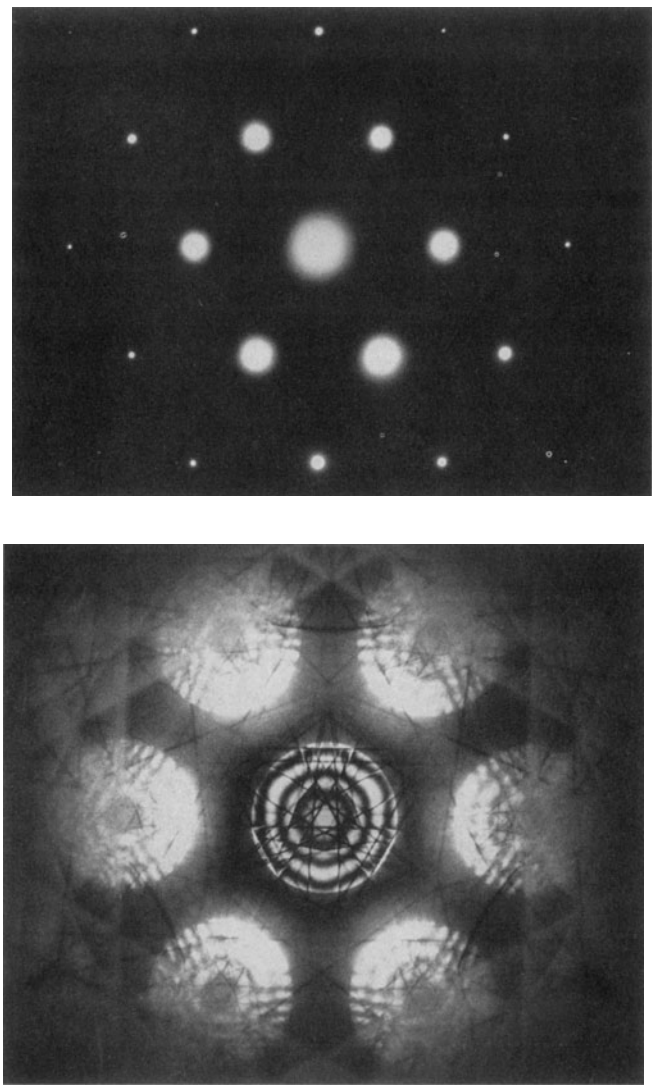

Figure 20.2. (A) SAD pattern from [111] Si showing the first few orders of diffraction spots but no Kikuchi lines. (B) CBED pattern from [111] Si showing dynamical contrast within the disks as well as Kikuchi and other lines.

From Figure 20.1 you can see that we need a strong upper-objective polepiece to create a convergent beam, so any probe-forming instrument, such as a TEM/STEM or dedicated STEM, can generate the patterns. Before the development of STEMs, CBED was possible by the addition of a mini-lens below the C2 lens of a conventional TEM, but then parallel-beam TEM imaging was impossible. We've already seen the detailed lens systems and ray diagrams associated with forming a convergent beam in Chapters 6 and 9, so here we will emphasize the experimental variables that you can control. We'll start with TEM mode and then describe STEM operation.

20.2.B. CBED in TEM

You can form CBED patterns in any TEM that is capable of creating a small (<< 1 μm) beam with a convergence semiangle (α) >10 mrads. This might not be possible on TEMs made before the late 1970s that do not have condenser-objective lenses, so you should check if your TEM is properly equipped before you spend a lot of time trying to get it to do something which won't be possible.

There are four microscope variables you need to control when forming a CBED pattern:

- The beam convergence semiangle α.
- The camera length (*L*) (i.e., the magnification).
- The focus of the pattern.
- The size of the beam.

When you focus the beam, you probably won't be able to see any useful image information, just a bright spot on the screen, but if the TEM is well aligned then the beam will be focused on the region you chose. You will develop your own procedure as you gain experience. Basically the approach is as follows:

- Start with your specimen in the eucentric plane, as usual, and form a focused image on the TEM screen with the area that you want to examine approximately in the middle of the screen.
- Select a large C2 aperture about 100–200 μm in diameter, carefully center it, then adjust the C2 lens to form a focused spot on the area of interest.
- Keep C1 weakly excited to give a relatively large spot, about 100–200 nm FWTM (see Chapter 5), containing sufficient current to give high intensity in the pattern.
- Select a small camera length, <500 mm, to give a wide-angle view of the pattern.
- To observe the CBED pattern just switch to diffraction mode, making sure the objective and SAD apertures are retracted.

Remember that you control the minimum illuminated area on the screen (i.e., the beam diameter at the specimen) by the strength of the C1 lens.

20.2.C. Choosing the C2 Aperture

Once the CBED pattern is visible you can adjust the convergence semiangle α by changing the C2 aperture, making sure to center the aperture you finally choose. The size of the diffraction disks depends on α, as shown in Figure 20.3.

The pattern of nonoverlapping disks is a Kossel–Möllenstedt (K–M) pattern.

To get such a pattern you must select a C2 aperture such that $2\alpha < 2\theta_B$ for the particular specimen and orientation. Typically, the Bragg angle is a few milliradians, and C2 apertures in the 10–50 μm range will usually ensure that you have satisfied the K–M conditions; we usually operate in this mode. If 2α is large enough for substantial overlap of the disks to occur such that individual diffraction maxima are no longer discernible, then the term "Kossel pattern" may be used (although this can cause confusion with the classical use of the term for geometrically similar X-ray patterns). Figures 20.3A–C show a series of

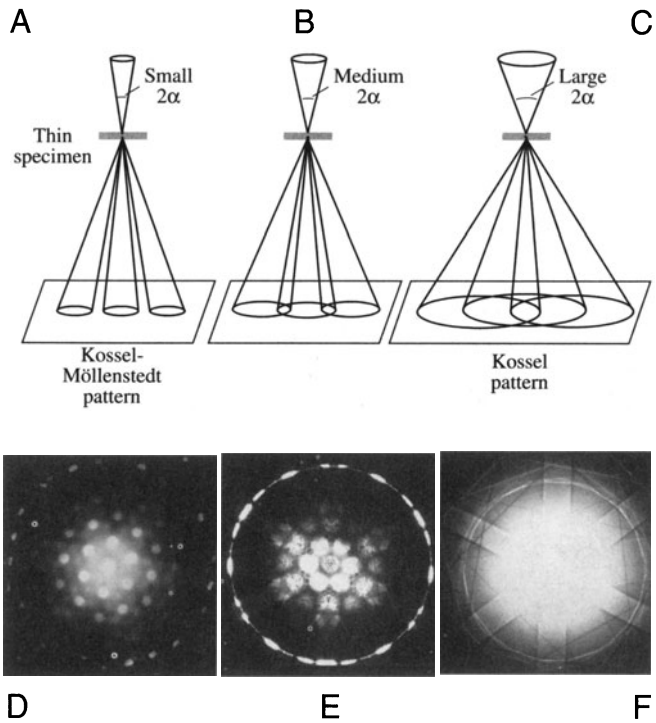

Figure 20.3. (A)–(C) Ray diagrams showing how increasing the C2 aperture size causes the CBED pattern to change from one in which individual disks are resolved to one in which all the disks overlap. In (D)–(F) you can see what happens to experimental patterns on the TEM screen as you select larger C2 apertures.

ray diagrams illustrating the transition from a K–M pattern to a Kossel pattern by increasing 2α. Equivalent experimental patterns from pure Al are shown in Figures 20.3D–F. The patterns in Figure 20.3 were all taken at a small camera length and you can see rings of intensity which arise from electrons scattered to quite high angles (±10°). We'll return to these HOLZ diffraction effects in Section 20.3.

Kossel patterns are most useful when viewed with a small camera length (L) because they display an enormous area of reciprocal space, and the large 2α gives rise to strong Kikuchi bands. The Kikuchi bands intersect at the zone axes in the center of the pattern, as you can see in Figure 20.3F, and therefore it is very easy for you to tilt to a particular zone axis. So, to form a ZAP, it is best to start at very small L with a large 2α. Later, you can worry about the best choice of C2 aperture and focusing the pattern.

Because we need to be able to vary α, a range of C2 apertures from about 10 μm up to 200 μm is desirable, consistent with the needs of other techniques. A reasonable choice of three C2 apertures comprises one of about 200 μm for routine TEM, EELS, and Kossel patterns, a 50–70 μm ultrathick aperture for XEDS (which can also be used for STEM imaging and some K–M patterns), and a 10–20 μm aperture for most K–M patterns. Some TEMs provide more than three apertures. More is better!

Because the C2 lens is excited in TEM mode, you can use it to change α, but if you do, the objective lens has to be changed also to maintain a focused pattern. You need to adjust C2 if you change the beam size with the C1 lens or if you want a value of α between those given by the fixed C2 apertures.

> Use the specimen height (z) control to maintain the specimen in the eucentric plane as you tilt. A computer-controlled stage is ideal for this.

If you need to know the value of α, you should use a known crystal to calibrate its variation with C2 aperture size for typical C2 lens excitations, as we described back in Section 9.1.

20.2.D. Choosing the Camera Length

The choice of L depends on the information that you want to obtain from the pattern. (Remember that L controls the magnification of the DP and a *large* L gives a *high* magnification view, but only spans a *small* angular range.) Typically we choose $L > 1500$–6000 mm to observe detail in the 000 (BF) disk at the highest possible magnification, and $L < 500$ mm to view the low magnification pattern, sometimes called the "whole pattern" (WP), containing electrons scattered to high angles. Figure 20.4 shows a series of CBED patterns obtained over a range of L and you can see that if we start at a high L (Figure 20.4A) we first see only the 000 disk and then the disks that are equivalent to an SAD pattern, but at smaller L the HOLZ effects that we just mentioned become visible (Figure 20.4C). Ultimately, at the smallest L, the angular range of the pattern is limited by the bore of the objective lens polepiece.

20.2.E. Focusing Your Pattern

If you don't focus your patterns you will miss a lot of the fine detail! First, the beam has to be focused in the speci-

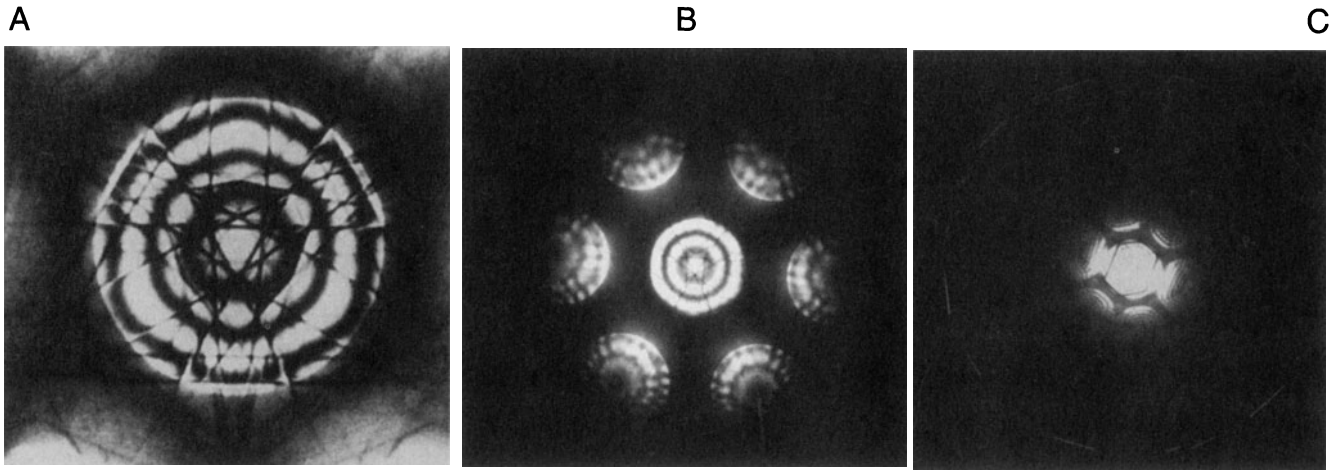

Figure 20.4. Decreasing the camera length expands our view of reciprocal space. (A) Starting at high L with a CBED pattern containing the 000 diffraction disk we then begin to see in (B) the distribution of electrons in the zero-order Laue zone. At the lowest camera lengths (C) the higher-order Laue zone is faintly visible. Typically, we can record electrons scattered over an angular range of ±10°.

men rather than underfocused or overfocused. The easiest way to find focus in TEM mode is to leave the objective lens alone and adjust the C2 lens to form the smallest spot on the TEM screen. Changing C2 thus also changes α, and if you want to maintain a fixed α then you need to adjust the objective lens strength as follows:

- Select K–M conditions and choose a value of L so you can clearly see the 000 disk.
- Deliberately overfocus (strengthen) the objective lens until a BF image is visible in the disk. This is because the beam is spread at the plane of the specimen (see Figure 20.5A and the associated ray diagram back in Figure 6.5A).
- Weaken the objective lens. As the beam crossover moves toward the specimen plane, the image expands to higher magnifications until it goes through an inversion point at exact focus (Figure 20.5B and Figure 6.5B).
- Underfocus, and again you can see a BF image in the 000 disk, inverted with respect to the overfocused image (Figure 20.5C and Figure 6.5C). As you can see in Figure 20.5B there is nonspatial (i.e., diffraction-contrast) information in the 000 disk when you are at focus. Know the value of the objective lens current that focuses the beam at the eucentric plane in your TEM. If your CBED pattern is focused at a different value, then adjust the lens current and refocus with the z-control to maintain eucentricity.

If you leave the objective lens current fixed and focus the beam on the specimen by adjusting C2, you'll see a similar effect to that shown in Figure 20.5. If you use the second (noneucentric) tilt axis, or move to another region of the specimen, you will probably have to refocus the pattern with the z-control.

The CBED pattern also has to be correctly focused in the back focal plane and you can do this in the conventional manner using the intermediate lens fine focus to sharpen the image of the C2 aperture.

Note that this operation is equivalent to creating multiple DF images with a parallel beam, which we used to calibrate the SAD pattern rotation in Section 9.6.C.

20.2.F. Choice of Beam Size

The last TEM variable is the beam size. We've already mentioned that you should start with a reasonably large beam to give a good intense pattern on the screen. Of course, a large beam size doesn't help if the crystal you're trying to analyze is small. The volume sampled by the beam

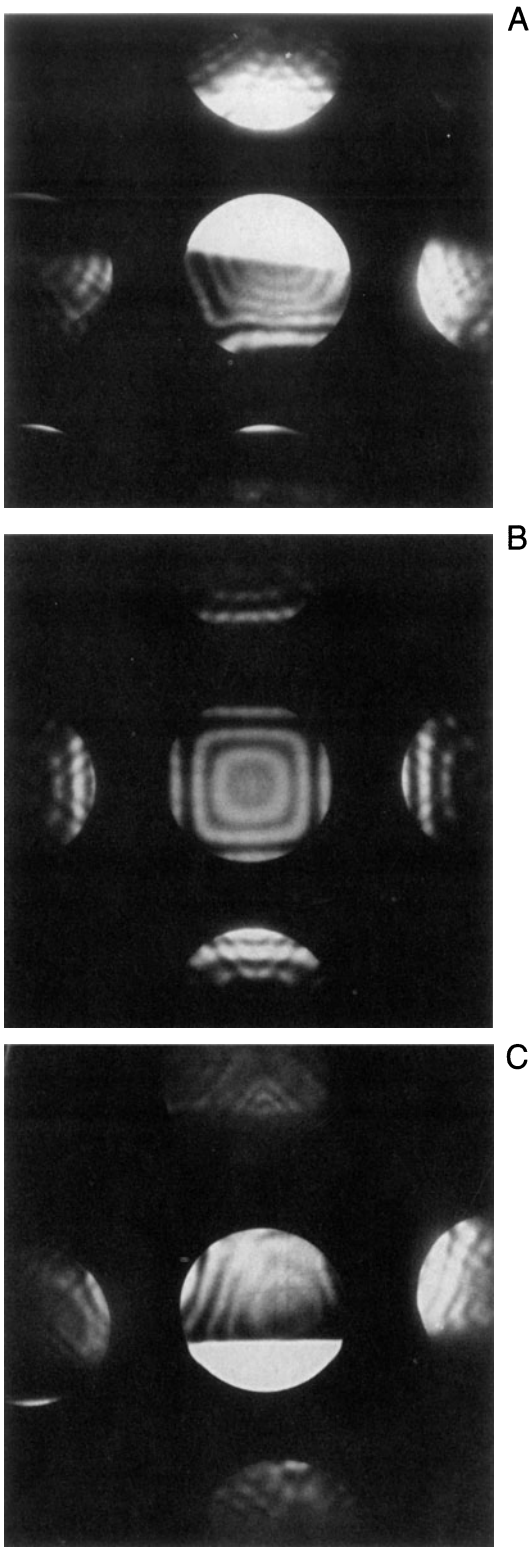

Figure 20.5. The procedure for correctly focusing the CBED pattern by adjusting the strength of the objective or C2 lens. In both overfocus (A) or underfocus (C) conditions you see a BF image in 000 and DF images in the $hk\ell$ disks, but at exact focus (B) the disks contain nonspatial dynamical-diffraction contrast.

defines the spatial resolution and so it is important to control the beam diameter. For the thinnest specimens, spatial resolution is close to the beam size, but in thicker specimens elastic scatter will spread the beam and degrade the resolution in a manner identical to XEDS (see Chapter 36). Using the thinnest specimens and an FEG, CBED patterns can be obtained from extraordinarily small regions, as we'll see in Section 21.8. Figure 21.15 shows that subnanometer diffraction is possible. However, there is a drawback to using the thinnest specimens because they don't exhibit dynamical-diffraction effects, as you'll now see.

20.2.G. Effect of Specimen Thickness

If your specimen is very thin you may have kinematical-diffraction conditions. Then the diffraction disks are uniformly bright and devoid of contrast, as shown in the ZAP in Figure 20.6A. Moving to a thicker area of the specimen in the same orientation transforms the pattern from an array of uniformly intense disks to a display of strong dynamical contrast (Figure 20.6B), which we'll discuss later. So to get the most out of a CBED pattern the specimen should be thicker than one extinction distance (see Chapter 16). This requirement differs from that of many other TEM techniques, such as HRTEM, XEDS, and EELS, where the best information is obtained from the thinnest specimens. So with CBED, you can almost always get something out of your specimens, even if they are too thick for anything else!

20.2.H. Final Adjustment

Sometimes it is quite difficult to make the ZAP exactly symmetrical as in Figure 20.2B. It often seems as if the last minor tilt or traverse of the specimen is not precise enough, or mechanical backlash occurs. If this is the case, use the beam tilts or deflectors to make your final adjustments to obtain a symmetric pattern. In Section 18.2 we used the same method to excite high-order reflections in SAD. You can also move the C2 aperture and center it on the zone axis, but this misaligns the illumination system, so it should only be a last resort.

As with SAD patterns, a range of exposure times for all CBED patterns will give you the most information.

20.2.I. CBED in STEM Mode

You should first get a focused STEM image of the specimen, as we described in Section 9.4.

The procedure is then quite simple:

- First stop the beam scanning (i.e., select "spot" mode on the STEM console).
- Position the spot on the STEM screen on the region of interest.

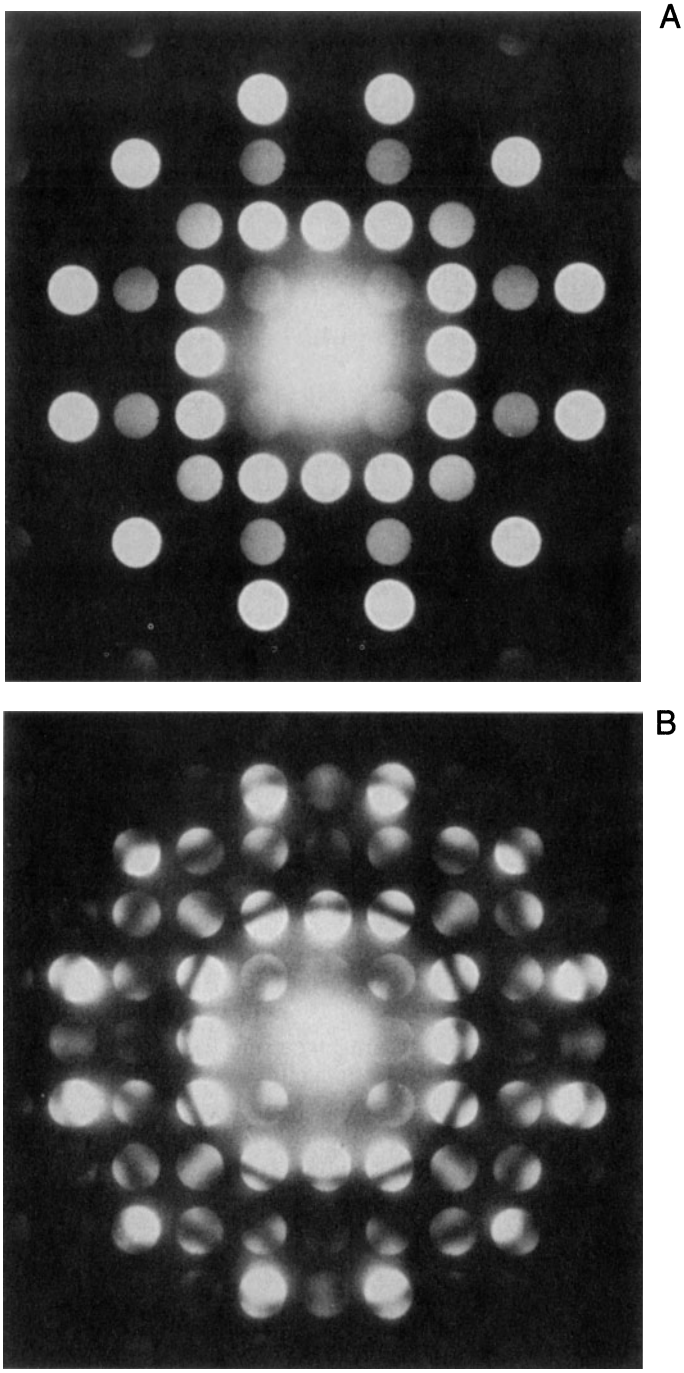

Figure 20.6. (A) [001] CBED pattern from σ phase in 316 stainless steel under kinematical conditions. Such patterns give us no more information than SAD. Their only advantage over SAD is that they come from a smaller region of the foil. (B) CBED pattern from a thicker area than in (A) showing dynamical-contrast phenomena.

A CBED pattern should then be visible on the TEM screen, but to see it you may have to remove the STEM detector if it sits above the TEM screen, or lower the TEM screen if the detector is below. The CBED pattern is present because the TEM is operated in the diffraction mode during STEM

operation. As before, you may have to reduce L to ensure that several diffraction maxima are visible on the screen. The other variables are the same, except that in STEM, the C2 lens in some TEMs is automatically switched off. This means that the C2 aperture alone governs α and you can only focus the pattern with the objective lens.

> In TEM, you can't see the area of the specimen you have chosen without spreading the convergent beam; in STEM, you can always scan the convergent beam to see the image.

In a DSTEM, you can see both image and DP at the same time because the CBED pattern can be viewed by introducing a screen after the last post-specimen lens and viewing this screen with a TV camera. A hole in the screen allows any selected portion of the pattern to travel through the EELS to the BF detector and thus both image and DP can be viewed simultaneously. If you don't have post-specimen lenses then you can't vary L; the CBED pattern is then viewed either directly using a TV camera looking at the back focal plane of the objective lens, or by scanning the pattern across the BF detector using post-specimen scan coils (see Section 21.7).

The choice of operating mode then is really up to you; TEM and STEM both have their advantages. We can now summarize the experimental steps to obtain a CBED pattern:

- Focus the beam to a crossover on your specimen at the eucentric plane and go to diffraction mode.
- Decrease L to see the full pattern including HOLZ scatter, and tilt to the desired orientation.
- Adjust the convergence semiangle with the C2 aperture.
- Increase the beam size if necessary with the C1 lens to make the pattern brighter.
- Increase L to look at the 000 disk and focus the pattern.

20.3. ZERO-ORDER AND HIGHER-ORDER LAUE-ZONE DIFFRACTION

20.3.A. ZOLZ Patterns

If you increase L above ~800 mm you will only see the first few diffraction maxima, as shown in Figure 20.2B. The CBED pattern consists of disks similar to the array of spots in an SAD pattern, i.e., discrete diffraction maxima surrounding the central 000 disk. Remember that such a pattern is termed a ZOLZ pattern since the permitted $hk\ell$ diffraction maxima must all satisfy the Weiss zone law relationship $hU + kV + \ell W = 0$, where UVW is the beam direction. Remember also that the $hk\ell$ maxima all lie in the reciprocal lattice plane containing the origin 000 of the reciprocal lattice, and this plane is also called the ZOLZ. So in fact SAD patterns are usually ZOLZ patterns, although we don't always describe them as such. From ZOLZ patterns we can obtain the usual interplanar spacings and angles and the $hk\ell$ maxima can be indexed and UVW identified, in exactly the same manner as for an SAD pattern. The two options, as we described in Section 18.4, are the method of ratios or a calibration standard to determine L.

Because of the finite size of the diffraction disks you must take care to select equivalent points in each disk when measuring the $hk\ell$ spot spacings. If α is too large, you might not see individual maxima and you should then select a smaller C2 aperture (K–M conditions).

20.3.B. HOLZ Patterns

The central bright portion of the CBED pattern is due to relatively intense low-angle scattering. At higher angles, the ZOLZ intensity drops because the atomic scattering amplitude, $f(\theta)$, has decreased. However, the intensity increases when the Ewald sphere intercepts the HOLZ planes in the reciprocal lattice and a ring of diffracted intensity is observed, as in Figures 20.3D–F and 20.4C.

> Remember that the radial distance from 000 in a DP is related to the angle of scatter; use a smaller L to see higher-angle scattering.

If you've chosen a small convergence semiangle, you'll see a ring of discrete HOLZ spots as in Figure 20.3D while a large C2 aperture gives a HOLZ ring of intersecting lines as in Figure 20.3F. The HOLZ intensity arises from weak high-angle diffraction from crystal planes that are *not* parallel to the beam. Low temperatures increase the HOLZ scatter and also minimize the thermal diffuse (phonon) scatter that in some materials masks the weak HOLZ intensity. So you'll find a liquid-N_2 cooling holder is often essential.

Consider the intersection of the Ewald sphere with the reciprocal lattice. The HOLZ planes in the reciprocal lattice cross the sphere, unlike the zero layer which is tangential to it, and the intersection of a sphere with a plane creates a ring. The first ring is called the FOLZ, because the possible $hk\ell$ reflections satisfy the relationship $hU + kV + \ell W = 1$, and so on. Where the Ewald sphere intersects these HOLZs, diffracted intensity is expected (taking into account the usual structure-factor effects; see next section). Because the beam converges on the specimen over an angular range 2α, the Ewald sphere is effectively rotated 2α

about the origin, and thus a range of angles in each HOLZ relrod is sampled, as shown in Figure 20.7A. This range of angles manifests itself in the CBED disk, sampling the intensity distribution along the relrod, as shown in Figure 20.7B. Different interception points on the relrod correspond to different points in the disk, also shown in Figure 20.7B. Figure 20.7C shows a typical experimental distribution of diffraction maxima from the Ewald sphere construction in Figure 20.7A. We've already shown similar experimental patterns, such as Figure 20.4C.

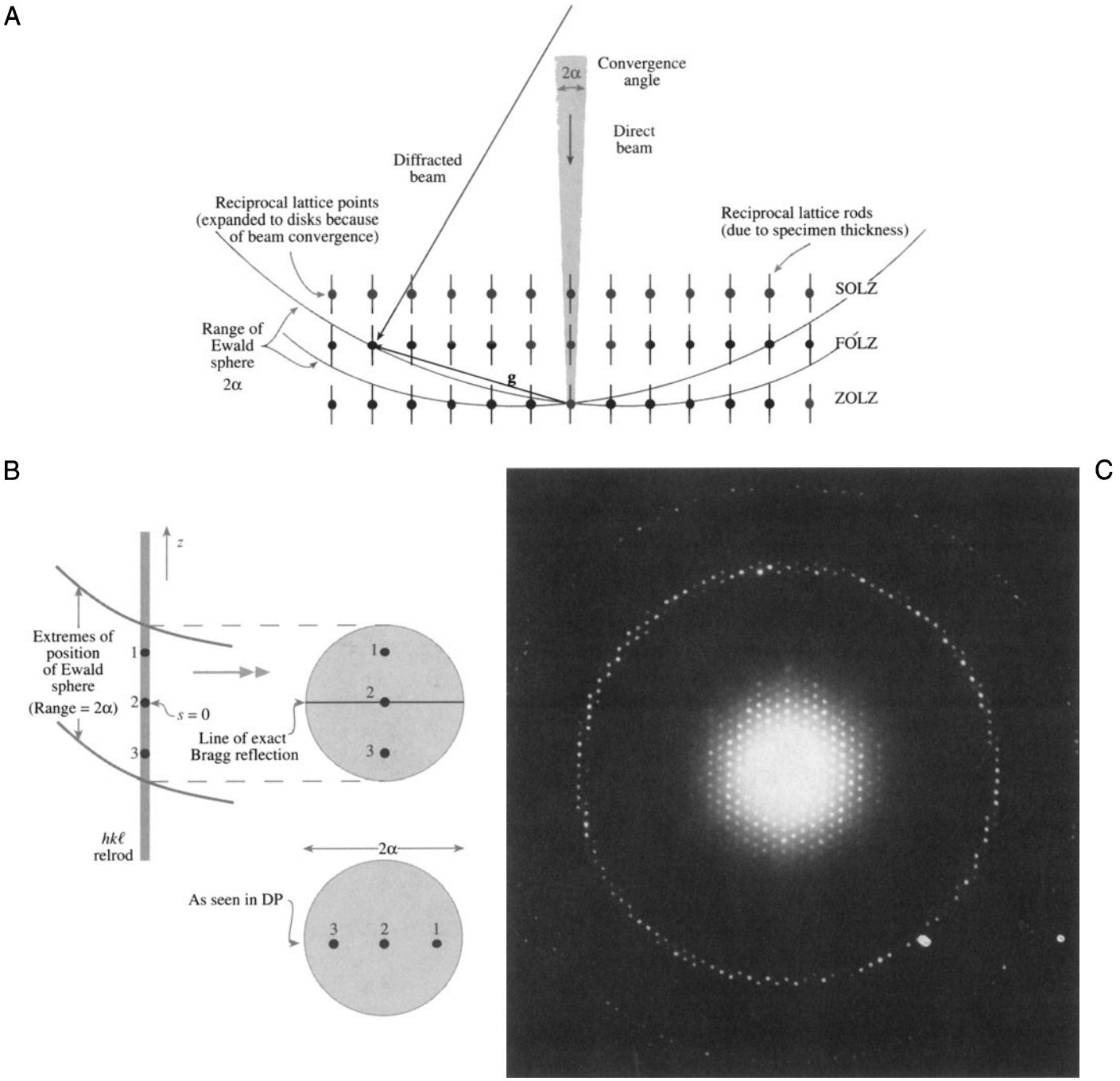

Figure 20.7. (A) The Ewald sphere can intercept reciprocal lattice points from planes not parallel to the electron beam whose **g** vectors are not normal to the beam. The sphere has an effective thickness of 2α because of beam convergence and so intercepts a range of these HOLZ reciprocal lattice points. The relrod has a shape shown in (B) and the intensity at specific points x_i in the relrod is directly related to equivalent points in the $hk\ell$ disk. The interception of the Ewald sphere with the HOLZ layers gives rings: the first ring is called the FOLZ, the second the SOLZ, and so on, shown experimentally in (C).

The most important point to remember immediately is that there is 3D crystallographic information in the CBED pattern whenever significant HOLZ diffraction intensity is present.

We'll make use of this 3D information in the next chapter.

To observe HOLZ rings in addition to the ZOLZ pattern, choose a very small L (<500 mm) so that you can see the full angular range of the back focal plane permitted by the imaging system (±10°). As shown schematically in Figure 20.7A, the Ewald sphere only intercepts reciprocal lattice points in HOLZs many orders of diffraction maxima away from the beam. Since the scattering into HOLZ spots is weak, the exposure time to reveal HOLZ maxima is usually long enough to ensure that the ZOLZ is overexposed on the negative (see Figure 20.7C). Therefore, you may have to record two DPs: a relatively short exposure for the ZOLZ pattern containing only two-dimensional crystallographic information, and a longer exposure for the weak HOLZ reflections containing the 3D information. As we've already said, a range of exposures is useful for *all* DPs.

There are some alternatives here:

- You can use careful photographic processing (Turner and Krishnan 1987) but you must plan this in advance.
- You might be lucky with your thin area; sometimes you can produce reasonable ZOLZ and FOLZ intensity on the same exposure (e.g., look ahead to Figure 20.16).
- A CCD camera will give a greater dynamical range, but perhaps with some minor loss of resolution.
- You can use image processing techniques to combine differently exposed patterns (see Chapter 30).

The HOLZ-ring radius is defined by the interception of the Ewald sphere with the allowed HOLZ relrods in the reciprocal lattice and so depends on the interplanar spacing in the crystal, the electron wavelength (i.e., the kV), L, and any off-axis lens distortion. Depending on the crystallography of the specimen, the HOLZ rings may have very large diameters, making them difficult to observe experimentally, even at very small L. Under these circumstances you should tilt to a *low*-symmetry zone axis (e.g., <114>) since this gives you a better chance of observing the FOLZ than a high-symmetry zone axis, such as <001>. (If the reason for this is not clear, then look at Figure 20.8.) If you still can't see a HOLZ ring, then the last thing you can try is increasing λ by lowering the kV.

In the next chapter, we will show you how HOLZ-ring measurements can be used to deduce the lattice-repeat vector of the crystal parallel to the beam direction. You can then determine the unit cell, the crystal system, and also the type of lattice centering.

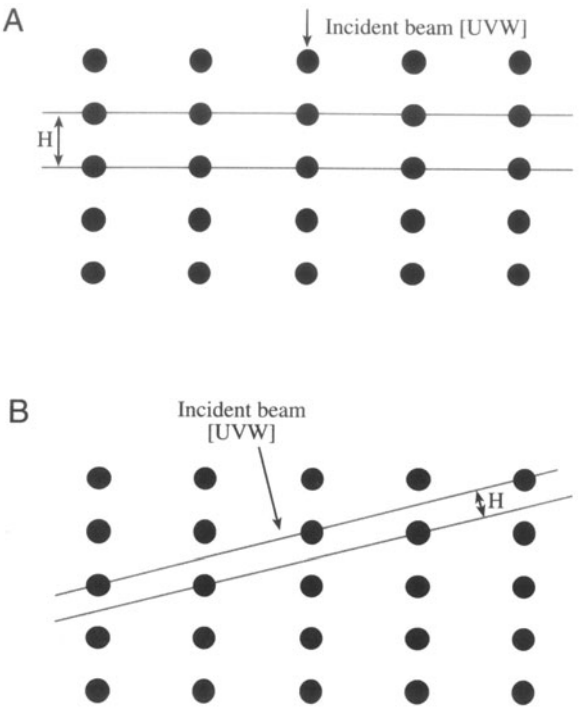

Figure 20.8. (A) The reciprocal lattice spacing (H) is large if the beam is down a major zone axis in the crystal. (B) The spacing is small if the beam is down a low-symmetry direction.

20.3.C. Indexing HOLZ Patterns

If you want to index the individual HOLZ reflections:

- Index the ZOLZ for which $hU + kV + \ell W = 0$ (see Section 18.4).
- Consult a stereographic projection to identify the poles of the principal planes constituting the FOLZ ($hU + kV + \ell W = 1$) and SOLZ ($hU + kV + \ell W = 2$), etc.
- Alternatively, you can just solve the Weiss zone law for the appropriate UVW.
- Check to see if the poles on the stereographic projection constitute allowed reflections.
- Index the HOLZ maxima.

If you want to make use of stereographic projections, see Chapter 18. Remember that the stereographic projection just gives you the major low-index $hk\ell$ planes and ignores any systematic absences.

Examples of indexed ZOLZ, FOLZ, and SOLZ patterns are shown in Figures 20.9A–C for the fcc lattice under (A) [001], (B) [110], and (C) [111] beam directions; Figures 20.10A–C show similar patterns for the bcc lattice.

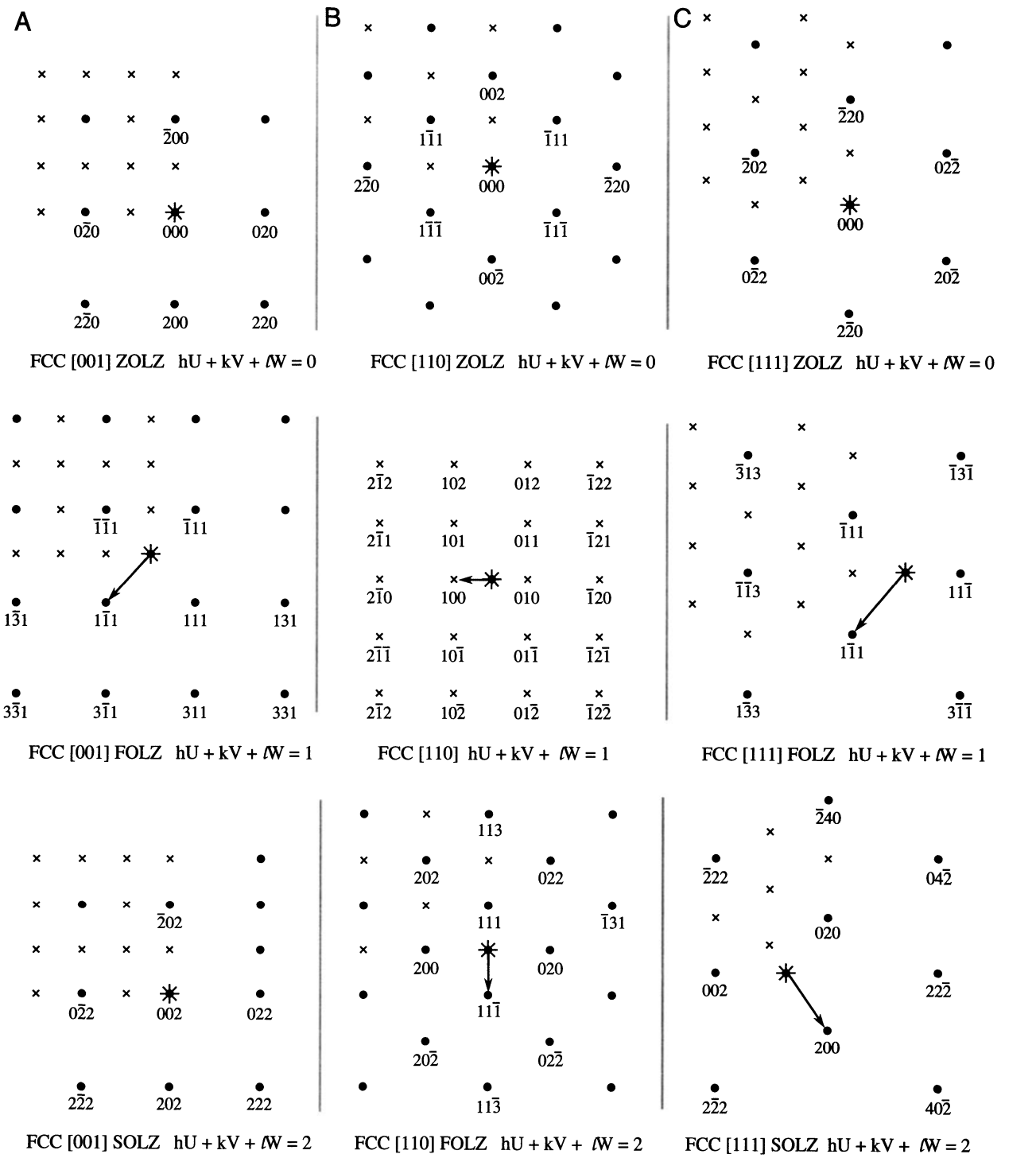

Figure 20.9. The possible ZOLZ, FOLZ, and SOLZ reflections for the three principal zone axes of an fcc specimen. Allowed reflections are shown as dots, forbidden reflections as crosses, the direct-beam direction is a star, and the arrow indicates the displacement vector between the ZOLZ and FOLZ. Note that when all reflections are forbidden for hU + kV + lW = 1 the FOLZ has hU + kV + lW = 2.

Only the first few orders of diffraction maxima are shown in each case. In practice, relatively high orders of diffraction maxima are present in the HOLZs, and the schematic patterns should be extended accordingly to match up with the experimental patterns (see Ayer 1989). From the schematic HOLZ patterns in Figures 20.9 and 20.10 you can see that the symmetry of each *UVW* zone is retained in each HOLZ pattern, but the HOLZ patterns are often shifted by a displacement vector relative to the ZOLZ because there is no allowed reflection on the zone axis. This

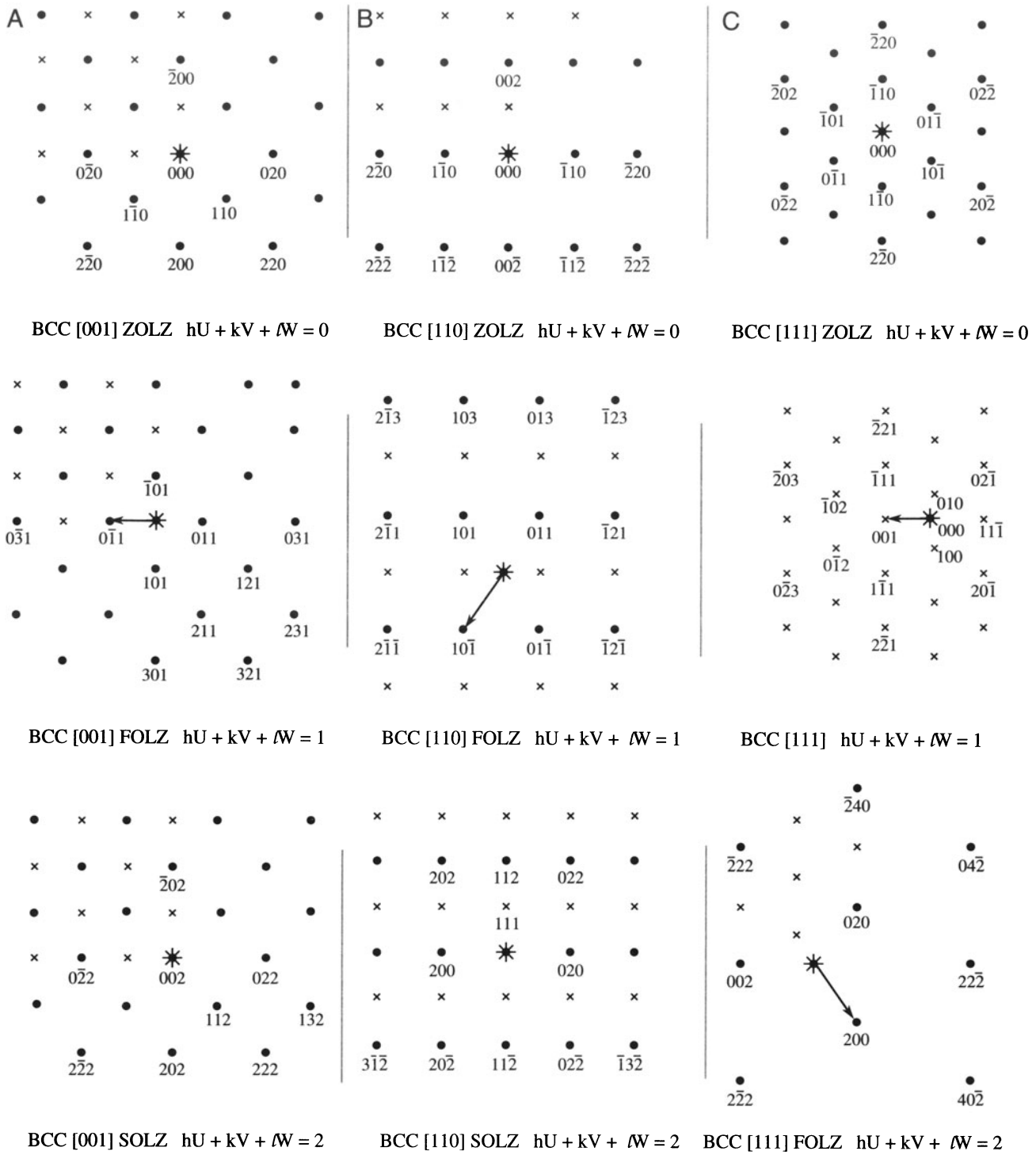

Figure 20.10. The possible ZOLZ, FOLZ, and SOLZ reflections for the three principal zone axes of a bcc specimen. Allowed reflections are shown as dots, forbidden reflections as crosses, the direct-beam direction is a star, and the arrow indicates the displacement vector between the ZOLZ and FOLZ. Note that when all reflections are forbidden for hU + kV + lW = 1 the FOLZ has hU + kV + lW = 2.

displacement can be calculated for any zone axis using equations which we'll discuss in the next chapter.

You should generate similar diagrams for the major zone axes of any specimen that you are going to study by CBED techniques; several computer programs, including EMS and Digital Microscopist, can do this readily (Section 1.5). There is also freeware available on the WWW. You may have to generate less symmetrical patterns (e.g., [233] or [114]) since these give rise to HOLZ rings with smaller radii, in which HOLZ phenomena are easier to see.

Be aware when you are indexing HOLZ rings that structure factors can cause every reflection in a reciprocal-lattice layer to be forbidden.

Under these circumstances the first ring of spots to be observed is from the second layer of the reciprocal lattice *but it is still called the FOLZ.* Well-known examples are the $(110)_{fcc}$ and $(111)_{bcc}$ patterns. You can't predict the total absence of a ring of HOLZ reflections just from the crystal symmetry, but it does vary with orientation. For example, in rhombohedral α-Al_2O_3, which has trigonal symmetry, all HOLZ layers are present if the [001] beam direction is observed, but in other directions in this system, e.g., [121], [141], and [542], only every third Laue zone is present. A detailed explanation of this is given by Raghavan *et al.* (1984).

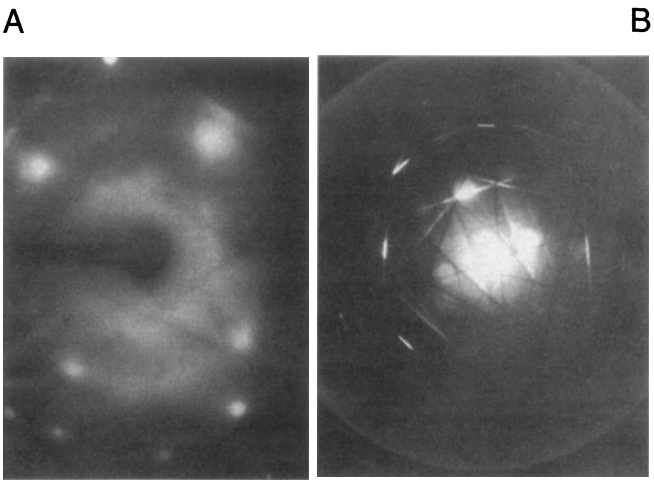

Figure 20.11. (A) Comparison of the poor quality of Kikuchi lines in an SAD pattern and (B) the relatively clear distribution in a CBED pattern from highly deformed copper.

20.4. KIKUCHI LINES IN CBED PATTERNS

In CBED patterns you almost invariably see sharp Kikuchi lines, while in SAD patterns Kikuchi lines are often rather diffuse or absent (see Chapter 19). This difference arises mainly because the convergent beam samples a much smaller region of the specimen than that selected by the SAD aperture. So in the volume of specimen contributing to the CBED pattern there is usually little or no strain, either elastic (due to specimen bending) or plastic (due to lattice defects). As a result CBED Kikuchi lines will, in general, be sharper. This effect is shown in Figure 20.11A, which is a conventional SAD pattern containing very diffuse Kikuchi lines. This pattern was obtained from a large region of deformed copper. By comparison, Figure 20.11B shows a CBED pattern from a much smaller region of the same specimen showing several pairs of well-defined Kikuchi lines. So you can use Kikuchi lines in CBED patterns to attack problems which are beyond the capability of SAD, for example, to determine accurate misorientation relationships between small grains in deformed materials (Heilman *et al.* 1983).

If the CBED pattern is not a ZAP, as in Figure 20.11B, the Kikuchi lines appear as pairs of excess (bright) and deficient (dark) lines, as in SAD patterns. But when you obtain a ZAP pattern, the ZOLZ Kikuchi lines appear as bright bands. These bands increase in intensity and definition as you increase the convergence semiangle, as shown in Figures 20.3D–F. A similar effect is seen in channeling patterns in the SEM which are generated by rocking a parallel beam around the optic axis. If you need to understand the difference between Kikuchi lines in SAD patterns and

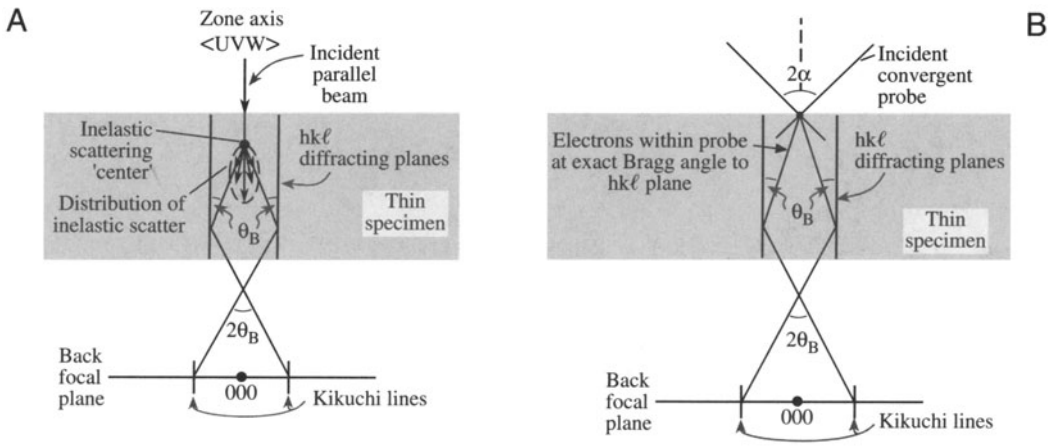

Figure 20.12. Comparison of the generation of Kikuchi lines (A) by inelastic scatter of electrons in a parallel beam and (B) by elastic scatter of electrons in a convergent beam when the convergence semiangle, α, is greater than the Bragg angle, θ_B.

Kikuchi bands in CBED patterns, Reimer (1993) gives a discussion.

The generation of Kikuchi lines in a CBED pattern is marginally more complex than in an SAD pattern. Remember how Kikuchi lines arise in a specimen illuminated by a parallel beam (see Chapter 19). In Figure 20.12 you can see what happens when a convergent beam is used. In this case the incident electrons span an angular range and therefore some electrons in the beam may already be at the Bragg angle to a ZOLZ plane. Thus, there will be an elastic-scattering contribution to the Kikuchi lines where they cross the disks in CBED patterns. If you choose Kossel conditions (i.e., $2\alpha > 2\theta_B$) as in Figure 20.12, there will always be electrons in the beam with the correct trajectory for exact Bragg diffraction from the planes in the *UVW* zone, and so there will *invariably* be an elastic contribution to the Kikuchi lines.

Strictly speaking, you should only use the term "Kikuchi lines" for the situation where inelastic scatter alone is responsible for their formation (i.e., the lines between any $hk\ell$ disks). However, the term is used rather loosely in the literature to describe the ZOLZ intensity bands, despite the elastic contribution to the scattered intensity.

20.5. HOLZ LINES

20.5.A. The Relationship between HOLZ Lines and Kikuchi Lines

Kikuchi lines also arise from inelastic scattering by the HOLZ planes and HOLZ Kikuchi lines exist in many CBED patterns. You can see the criss-cross array of deficient HOLZ Kikuchi lines between the ZOLZ maxima in Figure 20.2B. These HOLZ Kikuchi lines are in principle more useful than ZOLZ Kikuchi lines because they come from planes with much larger Bragg angles (and **g**-vectors), so they are more sensitive to changes in lattice parameter than the ZOLZ lines. Since

$$|\mathbf{g}| = \frac{1}{d}, \quad |\Delta\mathbf{g}| = -\frac{\Delta d}{d^2} \qquad [20.1]$$

So the smaller d, the larger $|\Delta\mathbf{g}|$ at the same Δd. We take advantage of this fact, not by using HOLZ Kikuchi lines specifically but by seeking out a closely related phenomenon called HOLZ lines. HOLZ lines are simply the elastic part of the HOLZ Kikuchi lines, that is, they are the part of the line which lies *within* the diffraction disks. By analogy with the production of Kikuchi lines, you can imagine that the lines arise when electrons within the incident beam at the correct Bragg angle for diffraction by a HOLZ plane are scattered out to high angles, creating a bright line through the HOLZ disk and leaving a dark line in the 000 disk. Not surprisingly, the theory for the origin of HOLZ lines is much more complicated than this. When you have time, you should read the paper by Jones *et al.* (1977).

As you see, the HOLZ lines come in pairs, like Kikuchi lines, with the bright (excess) lines within the HOLZ $hk\ell$ disks and the dark (deficient) lines within the 000 disk; an example of deficient lines is shown schematically in Figure 20.13. Because HOLZ lines contain 3D information, they show the true fcc threefold {111} symmetry while the ZOLZ Kikuchi lines and spots show sixfold two-dimensional {111} symmetry. We will make use of such differences when we discuss crystal-symmetry determination in Chapter 21.

20.5.B. Acquiring HOLZ Lines

Steeds (1981) has dealt with the practical problems of recording HOLZ lines in some detail. The main points you have to consider are:

- The lines are often only visible on the negatives and not on the screen, so you should record all the DPs, not just ones on which you can see the lines.
- You may have to make changes in the operating voltage or the orientation in order to view the HOLZ rings, especially if the crystal has a small reciprocal-lattice-repeat spacing parallel to the beam so the angular view of the back focal plane is poor.

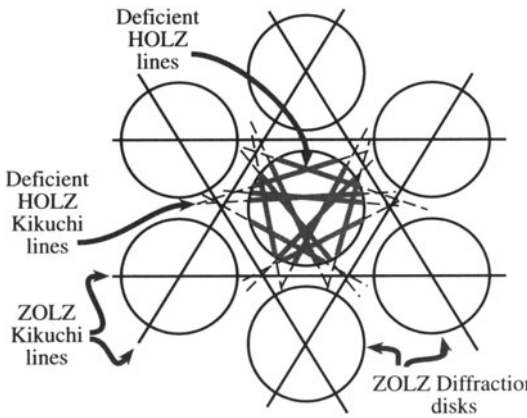

Figure 20.13. The relationship between Kikuchi lines and HOLZ lines is shown in this schematic of a [111] CBED pattern from an fcc crystal. The three principal pairs of $2\bar{2}0$ 110 ZOLZ Kikuchi lines show sixfold symmetry and bisect the **g**-vectors from 000 to the $2\bar{2}0$ ZOLZ disks. The inelastic HOLZ deficient Kikuchi lines are shown in the region between the ZOLZ diffraction disks and the elastic HOLZ deficient lines are present within the 000 disk only. Compare this schematic with the experimental pattern back in Figure 20.2B.

- Strains in the specimen from bending and thermal stresses smear out the HOLZ-line intensity. Choosing the smallest region (i.e., the smallest beam) may help this problem and will also minimize local thickness variations, but will lower the overall intensity of the pattern.
- Planar or point disorder as well as thermal effects can restrict large-angle scattering. In practice, this means that cooling the specimen and reducing the kV can help to increase HOLZ-line visibility; cooling also helps to reduce contamination and beam heating.
- Minor adjustments in HOLZ-line positions can help to distinguish HOLZ lines that overlap. To do this you need to change the kV by a small amount. So continuous kV control is an essential accessory if you're going to do serious CBED work.

The experimental procedure for observing HOLZ lines is quite straightforward, but since the lines themselves can be rather elusive, you should practice with a specimen such as silicon or stainless steel in which the lines are almost always visible. The best way to search for the lines is:

- Select the largest C2 aperture (largest 2α) and go to the smallest L at which you can see the full angular view of the back focal plane (about 500 mm).
- Examine the Kossel pattern, which should reveal Kikuchi line pairs intersecting at many poles, spanning a good fraction of the stereographic triangle as shown in Figure 20.14A.
- Tilt to a suitable zone axis. Remember, the best orientation for seeing the HOLZ lines is *not* a low-index, high-symmetry pole such as <100> or <111>, shown in Figure 20.14B, but a higher-index, lower-symmetry one such as <114>. One such pattern is shown back in Figure 20.3F.
- When you have tilted to a zone-axis orientation, you should see the ring of excess HOLZ lines.
- To see the deficient lines, increase L to look in detail at the 000 region of the pattern, and if necessary put in a smaller C2 aperture, center it, and look for the fine dark lines criss-crossing the bright disk as in Figure 20.14C. Usually you just need the deficient line distribution.

You have to use a range of L (from ~300 mm to 1500 mm) to obtain all this information, and this flexibility is only available on TEMs with more than three imaging lenses. DSTEMs with sufficient post-specimen lenses also offer this versatility.

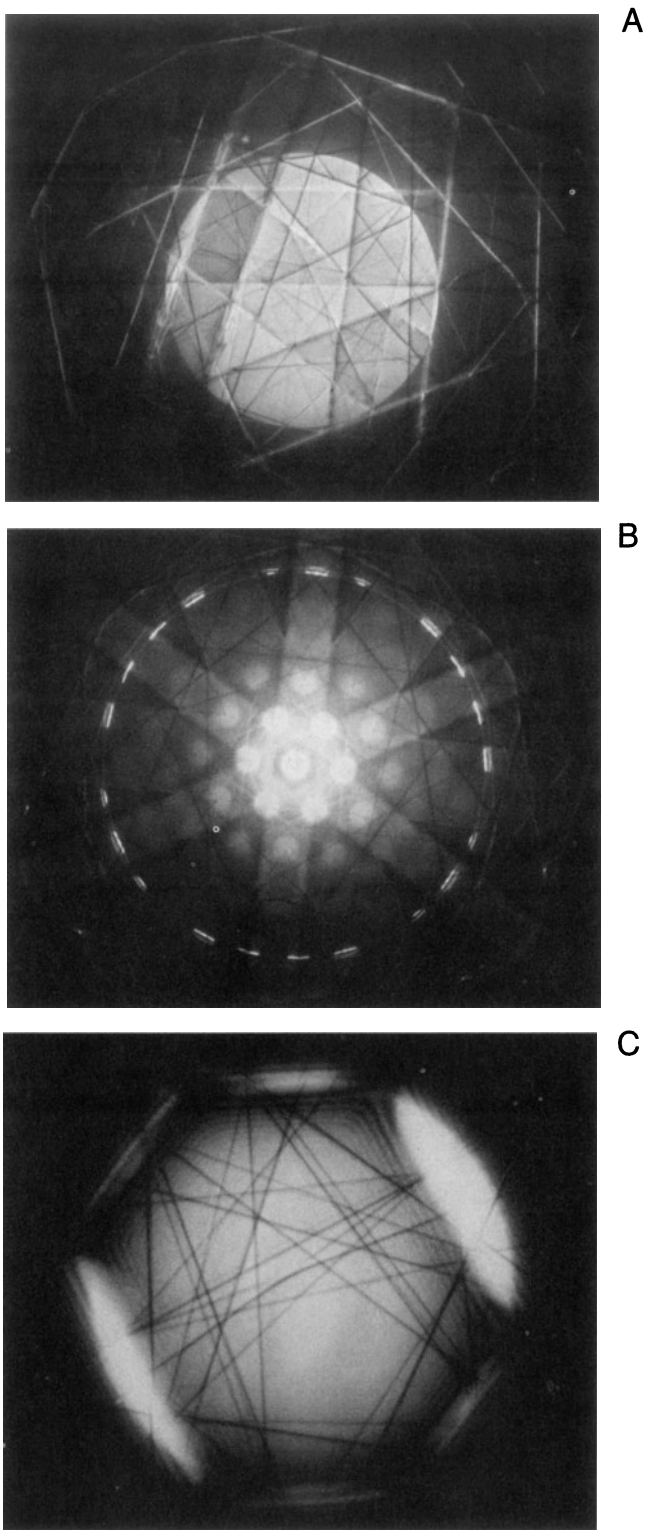

Figure 20.14. (A) Low L, large α CBED pattern showing a wide area of reciprocal space, away from ZAP conditions. (B) When the specimen is tilted to a low-index ZAP, and a smaller C2 aperture is inserted, a ring of excess HOLZ lines appears associated with the HOLZ disks. (C) Deficient HOLZ lines are visible in the central 000 disk of a low-symmetry 114 ZAP taken at high L.

20.5.C. Indexing HOLZ Lines

When you're recording the pattern containing the deficient HOLZ lines, you must also record another pattern with a small L and a small α to show the HOLZ disks: the first thing you have to do is index the HOLZ $hk\ell$ maxima in the manner we described in Section 20.4. Then observe which maxima show the clearest HOLZ excess lines. Each HOLZ line pair will be perpendicular to the **g**-vector from 000 to the HOLZ maximum. There should be a parallel HOLZ deficient line in the 000 disk, and this line can be assigned the same indices as the HOLZ maximum. If you repeat this exercise around the HOLZ ring most of the HOLZ lines should be indexed, as shown in Figure 20.15. Below the schematic pattern is a magnified drawing of the 000 disk and you should be able to see the association of each HOLZ line with a corresponding HOLZ maximum (Ecob *et al.* 1981).

In some cases you may find it difficult to associate a specific HOLZ deficient line in 000 with a specific HOLZ reflection due to strong excitation of two diffraction maxima. Under these circumstances, the two deficient lines may merge and appear to form a hyperbola. If you make small changes in the kV, the overlaps may resolve into two discrete lines. You should also be aware that faint HOLZ lines in the 000 disk may sometimes arise from second-order or third-order Laue zones; these very high-order lines are even more sensitive than first-order HOLZ lines to changes in kV and lattice parameter. The indexing of HOLZ lines lends itself to computer assistance and several programs have been described in the literature or are available on the WWW (for a review of which software is best, see Eades *et al.* 1993). Such programs can generate simulated HOLZ-line patterns for a given orientation, lattice parameter, and kV. Matching of the computer simulation with the experimental pattern then allows direct indexing. This procedure is also the first step in measuring the lattice parameter of the specimen and we will discuss this, along with other applications such as composition and strain measurements, in the next chapter.

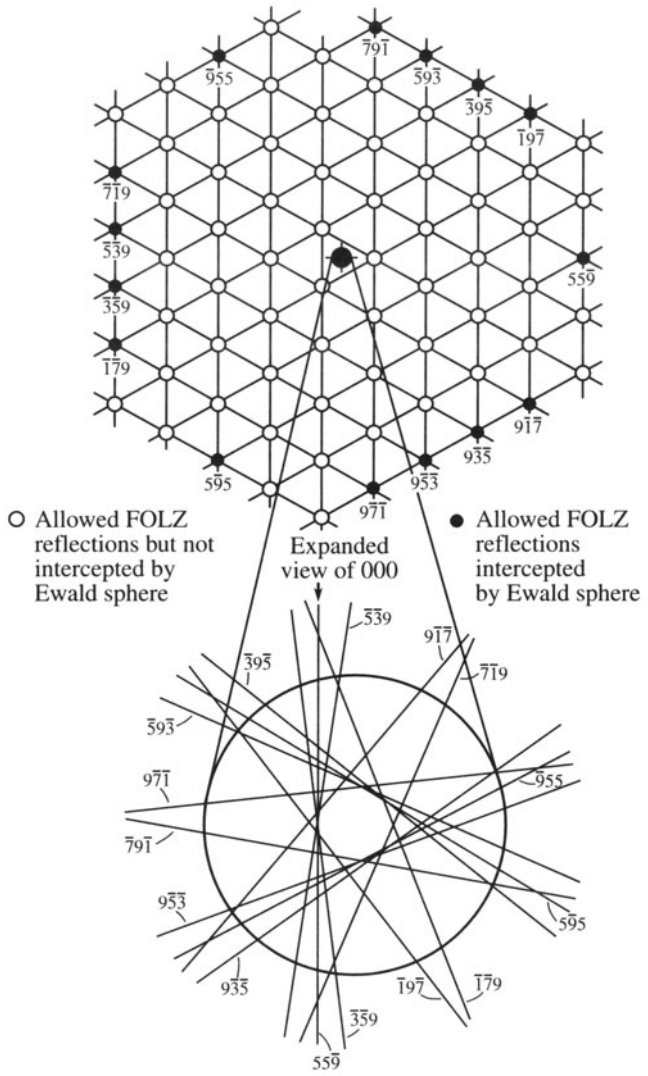

Figure 20.15. How to relate deficient HOLZ lines to the HOLZ maxima; the indexed FOLZ reflections in this [111] pattern are shown as full circles and the open circles are the rest of the FOLZ reciprocal lattice points that don't intercept the Ewald sphere. The **g**-vector from 000 to each $hk\ell$ FOLZ disk is normal to the $hk\ell$ HOLZ line and the lines are shown in the expanded 000 disk below.

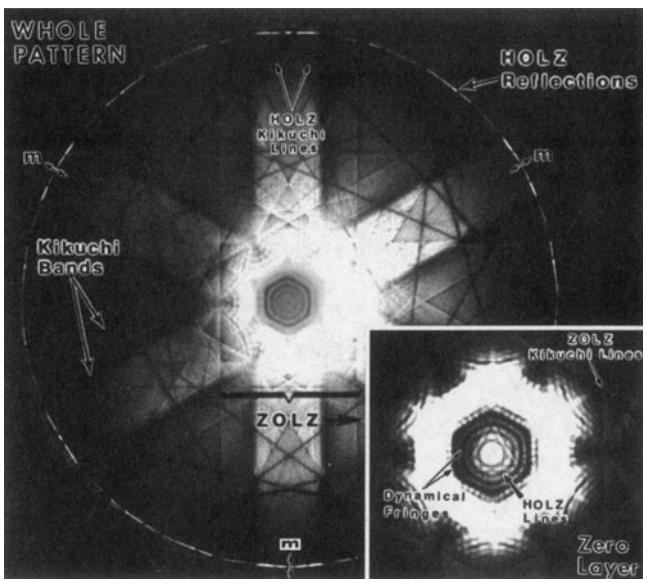

Figure 20.16. CBED pattern from Cu showing all the important characteristics. The ZOLZ pattern is visible, and the ZOLZ Kikuchi line pairs show six fold symmetry. The ring of excess HOLZ-line intensity can be seen. Deficient HOLZ lines in the 000 disk in the inset show only threefold symmetry and this symmetry difference will be exploited in the next chapter.

CHAPTER SUMMARY

In this chapter we've covered how to obtain different CBED patterns experimentally. Particular points and terms that you should know are:

- If you vary the specimen thickness, α, and L, then you can obtain CBED patterns showing many different features, particularly when the beam is down a zone axis.
- It is necessary to record patterns at different camera lengths with different exposure times.
- It is strongly recommended that you use a double-tilt cooling holder.
- You must be able to change the kV by very small steps, if you are studying HOLZ lines.
- Learn the meaning of such terms as ZAP, ZOLZ, FOLZ, HOLZ, and K–M and Kossel patterns.

If you look at Figure 20.16 you'll see many of the essential features of CBED displayed in one highly symmetrical pattern. In the next chapter we'll show you how to use this knowledge along with other aspects of CBED to get the maximum amount of crystallographic information from your specimen.

REFERENCES

General References

Loretto, M.H. (1994) *Electron Beam Analysis of Materials*, 2nd edition, Chapman and Hall, London.

Steeds, J.W. (1979) *Introduction to Analytical Electron Microscopy* (Eds. J.J. Hren, J.I. Goldstein, and D.C. Joy), p. 387, Plenum Press, New York.

Sung, C.M. and Williams, D.B. (1991) *J. Electron Microsc. Tech.* **17**, 95.

Williams, D.B. (1987) *Practical Analytical Electron Microscopy in Materials Science*, 2nd edition, p. 117, Philips Electron Optics Publishing Group, Mahwah, New Jersey.

Specific References

Ayer, R. (1989) *J. Electron Microsc. Tech.* **13**, 16.

Eades, J.A., Moore, S., Pfullman, T., and Hangas, J. (1993) *Microscopy Research and Technique*, **24**, 509.

Ecob, R.C., Shaw, M.P., Porter, A.J., and Ralph, B. (1981) *Phil. Mag.* **A44**, 1117.

Heilman, P., Clark, W.A.T., and Rigney, D.A. (1983) *Acta Met.* **31**, 1293.

Jones, P.M., Rackham, G.M., and Steeds, J.W. (1977) *Proc. Roy. Soc.* **A354**, 197.

Kossel, W. and Möllenstedt, G. (1939) *Ann. der Phys.* **36**, 113.

LePoole, J.B. (1947) *Philips Tech. Rundsch.* **9**, 33.

Raghavan, M., Scanlon, J.C., and Steeds, J.W. (1984) *Met. Trans.* **15A**, 1299.

Reimer, L. (1993) *Transmission Electron Microscopy; Physics of Image Formation and Microanalysis*, 3rd edition, Springer-Verlag, New York.

Steeds, J.W. (1981) *Quantitative Microanalysis with High Spatial Resolution* (Eds. G.W. Lorimer, M.H. Jacobs, and P. Doig), p. 210, The Metals Society, London.

Turner, J.H. and Krishnan, K.M. (1987) *J. Electron Microsc. Tech.* **5**, 211.